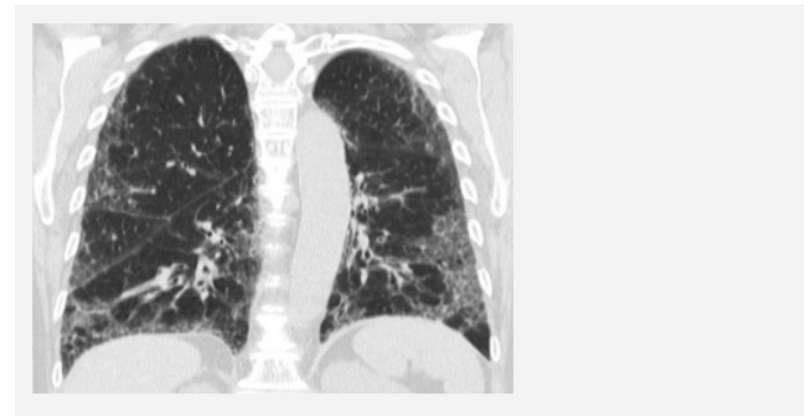


# Active epithelial Hippo signaling in idiopathic pulmonary fibrosis

Jason J. Gokey, Anusha Sridharan, Jenna Green, Gianni Carraro, Barry R. Stripp, Anne-Karina T. Perl, and Jeffrey A. Whitsett

# Introduction (1/4)

- Idiopathic pulmonary fibrosis (IPF):
  - Form of interstitial lung disease (ILD) resulting in alveolar remodeling and progressive loss of pulmonary function, respiratory failure and death within 5 years of diagnosis (1,2)
  - encompasses fibrotic remodeling, inflammation and loss of lung architecture (3)
- **Pathogenesis:** chronic, alveolar injury and failure to repair respiratory epithelium (4)
- **Histology:**
  - epithelial cells express atypical proximal airway epithelial and indeterminate cell type markers (5,6) including goblet cell characteristics that are normally restricted to conducting airways
  - fibrotic lesions and honeycomb structures replace alveolar structures (normally AT1 and AT2 cells)



Lungenfibrose: idiopathische pulmonale Fibrose (IPF); typisches radiologisches Bild einer Usual Interstitial Pneumonia (UIP) mit subpleural betonten Milchglasverschattungen, Honigwabengunge und Entwicklung von Traktionsbronchiektasen; Thorax-CT; oben: axialer Schnitt; unten koronaler Schnitt)

Ref: <https://www.caritasklinikum.de/kliniken-zentren/fachabteilungen-st.-theresia/kardiologie-pneumologie/einblick-in-unseren-alltag-schauen-sie-mal-rein/pneumologie-unsere-krankheitsbilder-im-roentgenbild>

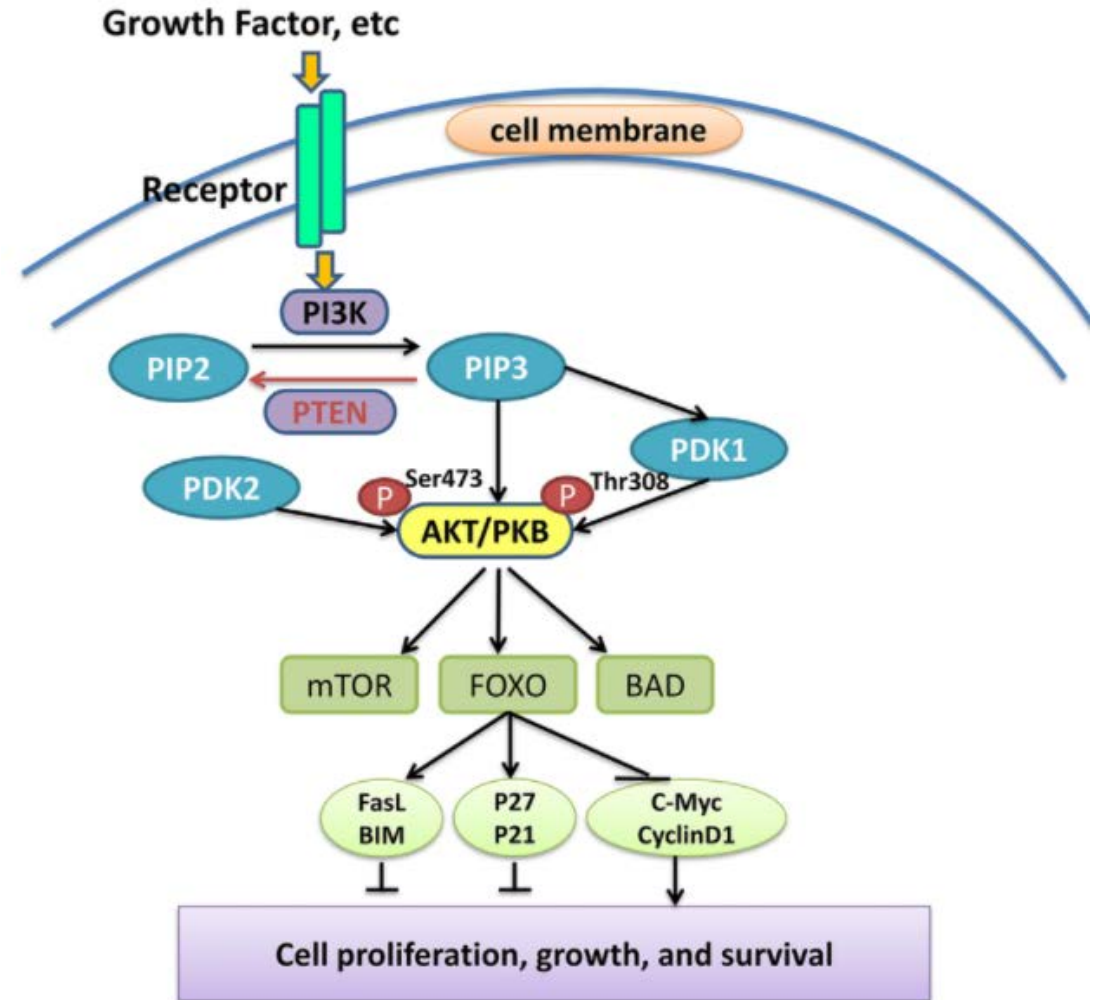
# Introduction (2/4)

- Transcriptomic analyses show dramatic changes in ciliated, basal and goblet cell-associated gene expression and loss of normal alveolar epithelial cells – profound changes in epithelial cell differentiation and function (6,7)
- Mutations affecting AT2 cell functions (ABCA3, SFTPA, SFTPB, and SFTPC) are among the genetic causes of chronic ILDs (8-11)
- In mouse models: chronically injured peripheral lung epithelial cells exhibit alveolar remodeling and fibrosis in association with activation of TGF-Beta (12), TGF-Alpha and the mTOR/PI3K/AKT pathways (13,14)

# Introduction (3/4)

- **single-cell RNA sequencing (RNAseq) of isolated respiratory epithelial cells:**
  - Identification of distinct populations of indeterminate, basal and goblet-like epithelial cells in IPF
  - identifying individual cells that shared RNA characteristics with AT2 cells and conducting airway epithelial cells consistent with a loss of normal cell-type lineage restriction (15)
- **Analysis of RNA profiles in IPF:**
  - activation of genes in the Hippo/YAP pathway, whereas inhibitors of the pathway, SAV1 and MST2 were suppressed
  - RNAs associated with activation of mTOR/PI3K/AKT signaling including increased MLST8 and decreased phosphatase and tensin homology (PTEN) expression were predicted in IPF epithelial cells (potential interactions between YAP and mTOR signaling pathways)

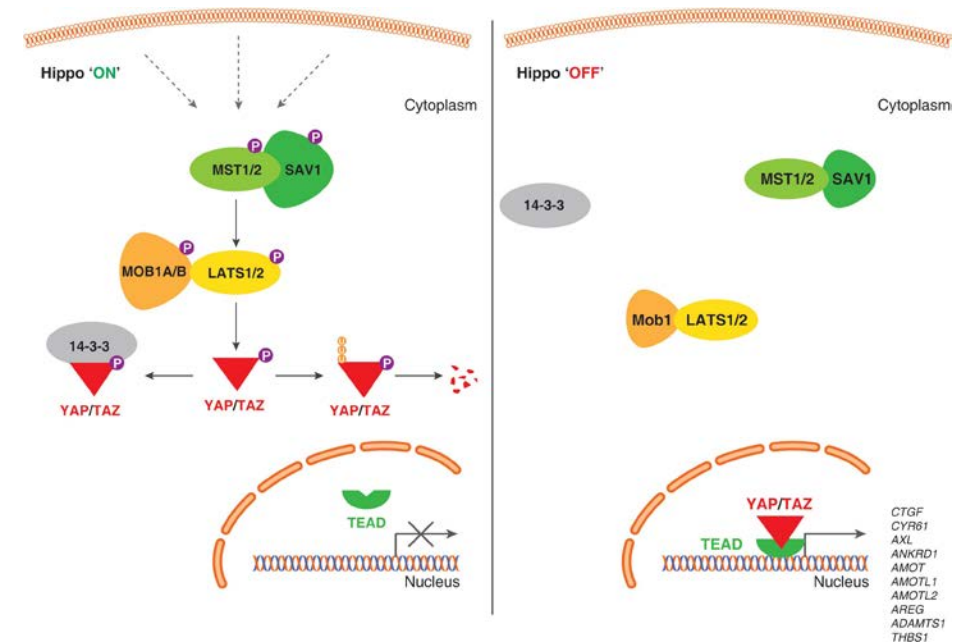
## mTOR/PI3K/AKT - pathway



Ref: [https://www.researchgate.net/figure/The-PI3K-AKT-FOXO-signaling-pathway-The-PI3K-AKT-pathway-is-the-canonical-pathway\\_fig1\\_329219442](https://www.researchgate.net/figure/The-PI3K-AKT-FOXO-signaling-pathway-The-PI3K-AKT-pathway-is-the-canonical-pathway_fig1_329219442)

# Introduction (4/4) – The Hippo signaling pathway

- Serine/threonine kinases Mst1 and Mst2 in concert with Salvador (Sav1) serve as YAP inhibitors by phosphorylating and activating large tumor suppressor kinases (Lats1 and Lats2)
- Lats1/2 phosphorylate downstream transcriptional effectors Yap and Taz to direct their cytoplasmic localization and inhibit transcriptional activities (16)
- In absence of inhibitory phosphorylation Yap/Taz translocate to nucleus and interact with transcriptional cofactors TEAD 1-4 to regulate target genes associated with cell proliferation, apoptosis and differentiation and induce known transcriptional targets including connective tissue growth factor (CTGF/CCN2) (17), AXL tyrosine kinase (18), and Ajuba (also known as JUB) (19)
- Ajuba inhibits activity of MST1/2 and LATs1/2 (counter regulator of the pathway) (20)
- YAP is required for normal branching morphogenesis and epithelial differentiation in the developing lung (24)
- Nucleus-localized YAP is required for airway epithelial cells to respond to TGF-Beta and controls SOX2 expression (25)
- Increased YAP activity in airway basal stem cells causes epithelial hyperplasia and impairs terminal differentiation, while YAP deletion causes terminal differentiation or the loss of the ability of basal cells to dedifferentiate into progenitor cells (25,26)
- Genetic deletion of MST1/2 in adult and fetal mice increased nuclear YAP, causing airway hyperplasia and abnormal differentiation of airway epithelial cells (19)



Boopathy, G. T. K., & Hong, W. (2019). Role of Hippo Pathway-YAP/TAZ signaling in angiogenesis. *Frontiers in Cell and Developmental Biology*, 7(APR), 49. <https://doi.org/10.3389/FCCELL.2019.00049/BIBTEX>

# Results (1/8)

## Activation of YAP-mediated gene expression in IPF

- RNAseq data from FACS isolated epithelial cells from normal and IPF, and primary human bronchiolar epithelial cells (HBECS) expressing activated YAP (S127A) was performed to predict the bioprocesses and pathways shared in these data sets
- Genes encoding proteins involved in mTOR, PI3K/AKT and Hippo/YAP and WNT signaling were predicted to be active by functional classification and network construction using ingenuity pathway analysis (IPA)
- Network analysis predicted extensive interactions among mTOR, PI3K/AKT, planar polarity and Hippo/YAP signaling
- **Hypothesis:** phenotypic features in IPF are regulated in part by activation of Hippo/YAP-associated signaling (Figure 1A)
- Gene expression changes include increased YAP1, JUB, AKT3, AMOTL2, GA6S, and CYP24A1 RNAs
- IPF epithelial cells and primary HECs expressing activated YAP (S127A) shared enriched bioprocesses including **extracellular matrix organization, cell migration, response to wound, cell size and epithelial proliferation/differentiation and increased expression of genes associated with canonical TGF-Beta, Hippo/YAP, and PI3K/AKT signaling pathways** essential for processes known to be regulated by the Hippo/YAP Pathway (16)

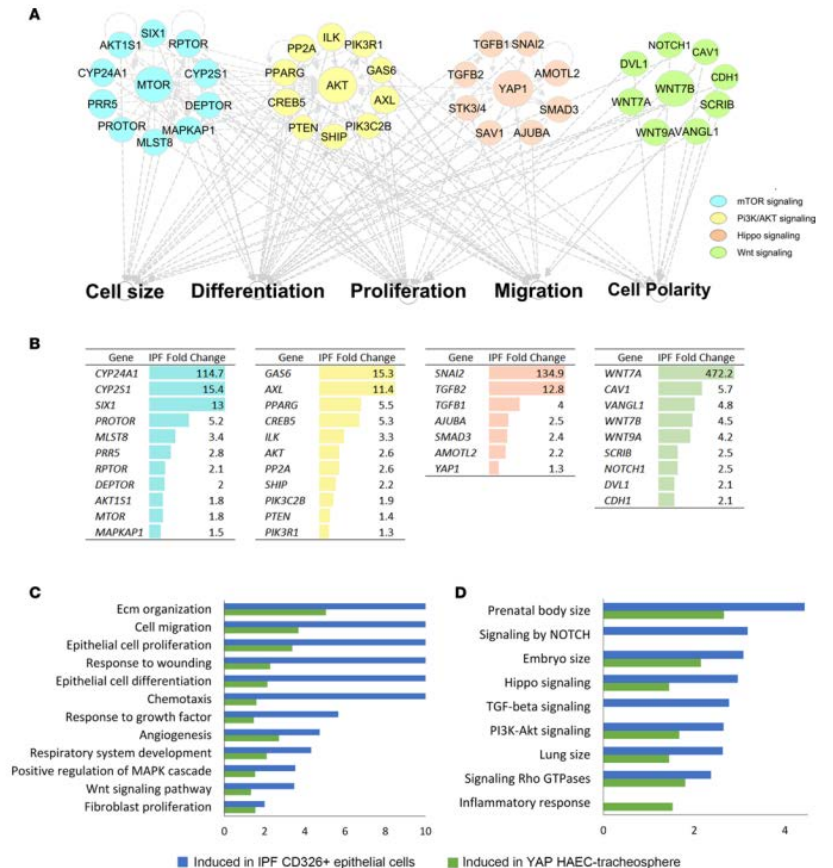
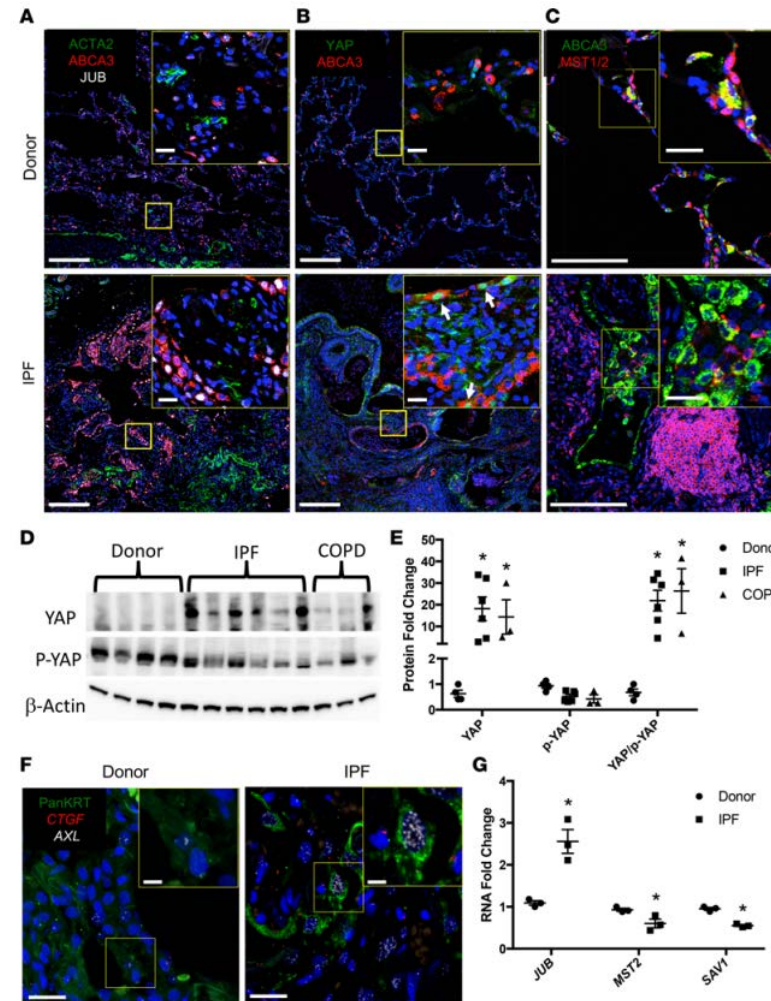


**Figure 1. Prediction of signaling interactions in idiopathic pulmonary fibrosis (IPF) epithelial cells.** (A) Ingenuity pathway analysis of RNA sequencing data from CD326<sup>+</sup>/HTII-280<sup>+</sup> sorted epithelial cells from healthy donors (n = 3) and IPF (n = 3) was used to predict intensive interactions among mTOR/PI3K/AKT, Hippo/YAP, and polarity signaling pathways. (B) Genes associated with each of the pathways significantly altered in IPF are shown. Each pathway is represented by a distinct color code: mTOR (blue), PI3K/AKT (yellow), Hippo (pink), and polarity (green). (C and D) Functional enrichment analysis predicted that genes induced in CD326<sup>+</sup>/HTII-280<sup>+</sup> IPF epithelial cells (8) and in human airway epithelial cells (HAECs) expressing YAP (20) share (C) commonly activated bioprocesses and (D) signaling pathways including those affecting epithelial cell proliferation, migration, and cell size. The x axis represents the -log10-transformed enrichment P value.

# Results (2/8)

## *Increased YAP activity in IPF epithelial cells*

- Immunofluorescence confocal microscopy and in situ hybridization RNA analyses of peripheral lung tissue demonstrated **increased nuclear YAP** and **decreased MST1/2 in IPF epithelial cells** that costained with ABCA3 or pan-cytokeratin
- Ajuba, a known transcriptional target of YAP, was increased and primarily detected in epithelial cells in IPF lesions (Figure 2, A-C)
- In normal donor lung tissues nuclear YAP was rarely detected, MST1/2 was highly expressed in alveolar AT2 cells
- Western blot analysis of whole-lung lysates demonstrated increased total YAP in IPF and chronic obstructive pulmonary disease (COPD) tissues, while levels of phosphorylated YAP were similar in normal, IPF, and COPD lung samples (Figure 2D).
- The ratio of total YAP to phosphorylated YAP was significantly increased in IPF compared with normal lung tissues, consistent with increased active YAP in IPF (Figure 2E).
- Proximity ligation fluorescence in situ hybridization (PLISH) was used to detect YAP target genes AXL and CTGF in IPF epithelial cells (Figure 2F):
  - AXL RNA was increased throughout the lung and particularly in epithelial cells.
  - SAV1 and MST2, inhibitors of YAP activity, were reduced, JUB was increased in RNA from CD326+ sorted IPF respiratory epithelial cells (Figure 2G).
  - Loss of the YAP inhibitors, SAV1 and MST2, and increased YAP target gene expression were consistent with increased YAP transcriptional activity in IPF epithelial cells.



# Results (3/8)

## *Epithelial cell polarity is disrupted in IPF*

- immunofluorescence staining of epithelial cell polarity markers scribble (SCRIB) and vang-like (VANGL) was performed to assess epithelial cell polarity in IPF
  - In contrast to apical localization in normal epithelial cells, SCRIB and VANGL staining was increased and diffuse (Figure 3, A and B), indicating loss of normal apical-basal polarity in IPF epithelial cells
  - VANGL1, SCRIB, and CELSR1 RNAs were increased in IPF epithelial cells, consistent with disruption of normal cell polarity in IPF (Figure 3C), and consistent with RNAseq data that demonstrated increased expression of cell polarity genes in IPF (Figure 3D).

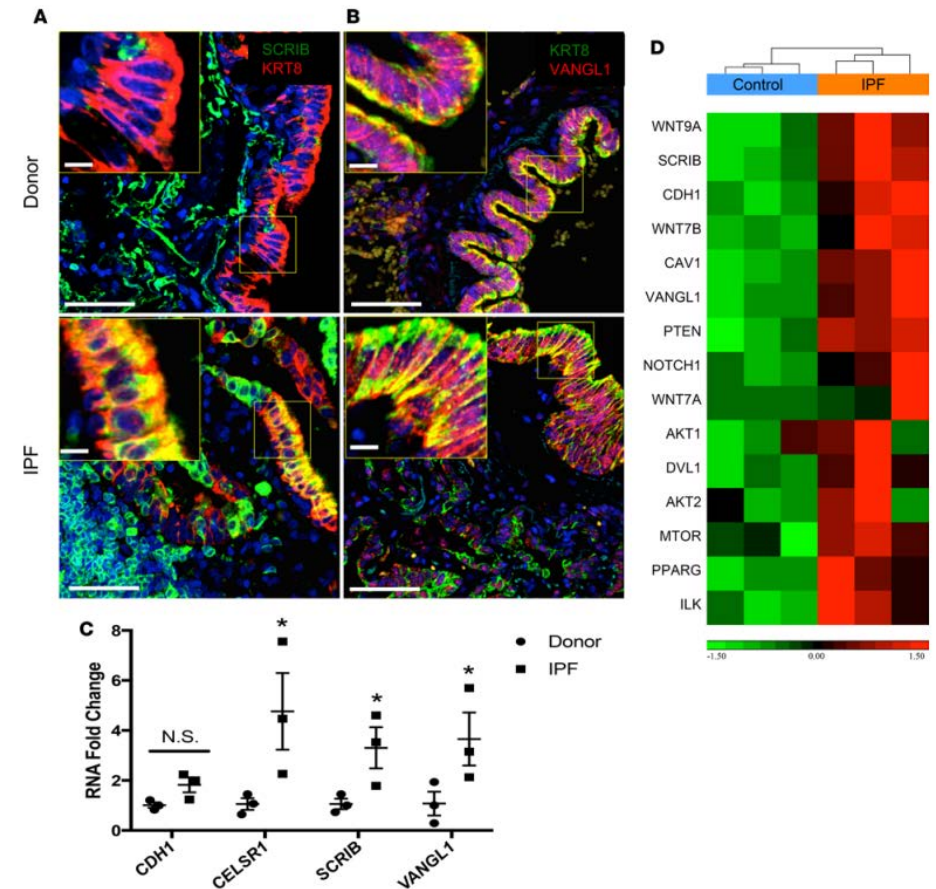


**Figure 3. Vangl and Scribble in idiopathic pulmonary fibrosis (IPF) lung tissue.** (A and B) Representative immunofluorescence imaging of healthy donor ( $n = 4$ ) and IPF ( $n = 6$ ) lung tissue are shown. (A) Scribble (Scrib) (green) and Krt8 (red) or (B) Vangl (red) and Krt8 (green). Scale bars: 50  $\mu\text{m}$  and 5  $\mu\text{m}$  (insets). (C) *CDH1*, *CELSR1*, *SCRIB*, and *VANGL1* RNAs were measured in CD326<sup>+</sup> sorted epithelial cells from healthy donors ( $n = 3$ ) and IPF ( $n = 3$ ) lungs. (D) RNA sequencing analysis of polarity-associated genes of healthy donors ( $n = 3$ ) and IPF ( $n = 3$ ) demonstrating significant increases in epithelial cell polarity genes including *WNT9A* and *WNT7A*. \* $P < 0.05$ , calculated by Student's *t* test. N.S., not significant.

# Results (4/8)

## *mTOR Increased activity in IPF respiratory epithelial cells and lung tissue.*

- immunofluorescence imaging was used to assess levels of phosphorylated S6 kinase (p-S6K), a downstream component of mTOR/PI3K/AKT signaling, in IPF epithelial cells (Figure 4A)
  - p-S6K staining was increased in IPF lung tissue and selectively increased in and colocalized primarily with pan-cytokeratin staining in IPF epithelial cells
- immunoblotting demonstrated increased p-PTEN, p-S6, and total S6 in IPF tissues compared with tissue from donors or COPD patients (Figure 4, B and C)
  - Increased expression of mTOR/PI3K/AKT components and inhibition of PTEN in IPF epithelial cells - increased mTOR activity.

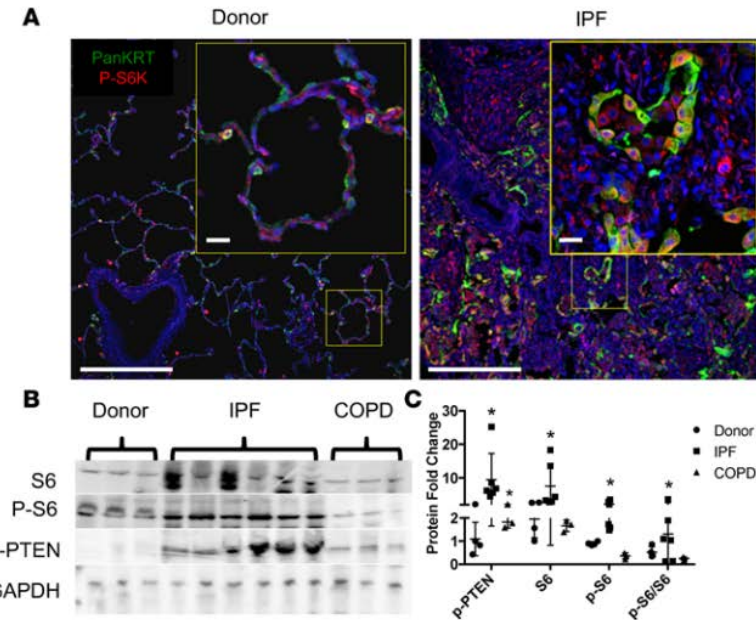
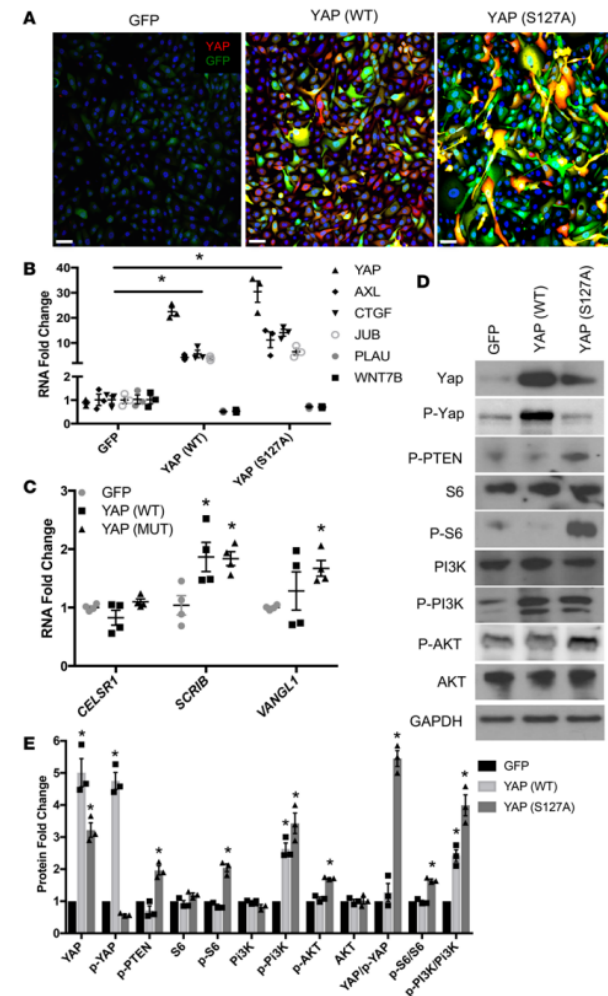


**Figure 4. Increased mTOR signaling in idiopathic pulmonary fibrosis (IPF) respiratory epithelium.** (A) Representative immunofluorescence imaging of healthy donor ( $n = 3$ ) and IPF ( $n = 3$ ) lung for phosphorylated S6K (p-S6K) (red) with pan-cytokeratin (Pan-KRT) (green) is shown. Scale bars: 50  $\mu\text{m}$  and 5  $\mu\text{m}$  (insets). (B) Representative immunoblots were prepared from whole-lung lysates of donor ( $n = 4$ ), COPD ( $n = 3$ ), and IPF ( $n = 6$ ) lung tissue for total S6, phosphorylated S6 (p-S6), and phosphorylated PTEN (p-PTEN). (C) Western blots were normalized to GAPDH. \* $P < 0.05$ , determined by ANOVA.

# Results (5/8)

## *YAP activates mTOR/PI3K/AKT signaling in HBECs*

- hTERT/CDK4-immortalized human bronchiolar epithelial cells (HBEC3KT, referred to as HBEC3) were transduced with lentivirus expressing YAP (WT) or constitutively active YAP (S127A)
- Immunofluorescence confocal microscopy demonstrated increased nuclear YAP after lentiviral transduction (Figure 5A)
- Western blotting and quantitative PCR (qPCR) analyses demonstrated increased YAP and YAP transcriptional target RNAs, i.e., JUB, AXL, and CTGF, consistent with activation of YAP (Figure 5B). YAP induced planar polarity genes SCRIB and VANGL1 (Figure 5C).
- Activated YAP (S127A) increased the phosphorylation of S6, PI3K, AKT, and PTEN, indicating that YAP activates the mTOR/PI3K/ AKT pathway in HBEC3s (Figure 5D).
- Expression of YAP (WT) increased p-PI3K but did not alter p-S6, p-AKT, or p-PTEN (Figure 5E). YAP-mediated induction of p-S6, p-PI3K, and inhibition of PTEN support the predicted interactions between YAP and mTOR/PI3K/AKT activity in IPF.



# Results (6/8)

## *Verteporfin inhibits YAP-induced targets, p-S6, cell proliferation, and migration.*

- Verteporfin inhibits YAP transcriptional activity by influencing YAP-TEAD interactions and is photoactivated (27)
- Verteporfin reduced nuclear YAP staining, total YAP expression, and inhibited p-S6 in HBEC3s (Figure 6A and Supplemental Figure 1A).
- Total YAP was reduced following verteporfin treatment in darkness (Figure 7A). YAP targets were significantly reduced regardless of light exposure (Figures 6B and 7B); however, in the absence of light, higher concentrations of verteporfin were required (Supplemental Figure 4).
- Verteporfin inhibited nuclear localization of YAP, total YAP mRNA, YAP target gene expression, and YAP-mediated cell migration.
- YAP-expressing cells were treated with verteporfin in the presence of proteasome inhibitor MG132 - protected YAP from verteporfin-induced degradation
- cells treated with verteporfin in the presence of mTOR activator MHY1485 - expression of YAP and p-S6 were increased; however, MHY1485 failed to block loss of YAP following verteporfin treatment (Figure 7B) - activated mTOR was not sufficient to prevent destabilization and inhibition of YAP by verteporfin

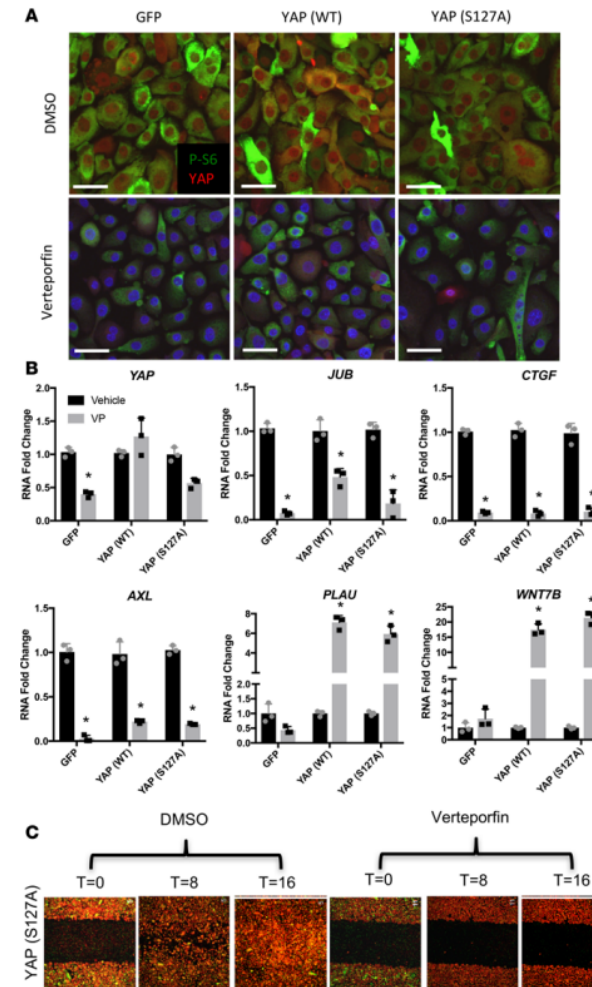


**Figure 6. Verteporfin inhibits YAP transcriptional activity and phosphorylation of S6 in ambient light.** HBEC3s were transfected with GFP, YAP (WT), or YAP (S127A) lentiviral vectors and treated with either vehicle (DMSO) or 0.25 μg/ml verteporfin for 48 hours (n = 3). **(A)** Immunofluorescence of p-S6 (green) and YAP (red) was assessed following verteporfin (0.25 μg/ml) or DMSO. Scale bars: 10 μm. **(B)** YAP, JUB, AXL, CTGF, WNT7B, and PLAU RNAs were quantified following 0.25 μg/ml verteporfin (VP) or vehicle exposed to ambient light (n = 3). Expression is normalized to DMSO controls. **(C)** Scratch assay of YAP (S127A)-transduced HBEC3s following DMSO or verteporfin treatment (0.25 μg/ml) in ambient light at T = 0, 8, and 16 hours of assay (n = 3). \*P < 0.05, determined by ANOVA. HBEC3s, hTERT/CDK4-immortalized human bronchiolar epithelial cells.

# Results (7/8)

## *Verteporfin inhibits YAP-induced targets, p-S6, cell proliferation, and migration.*

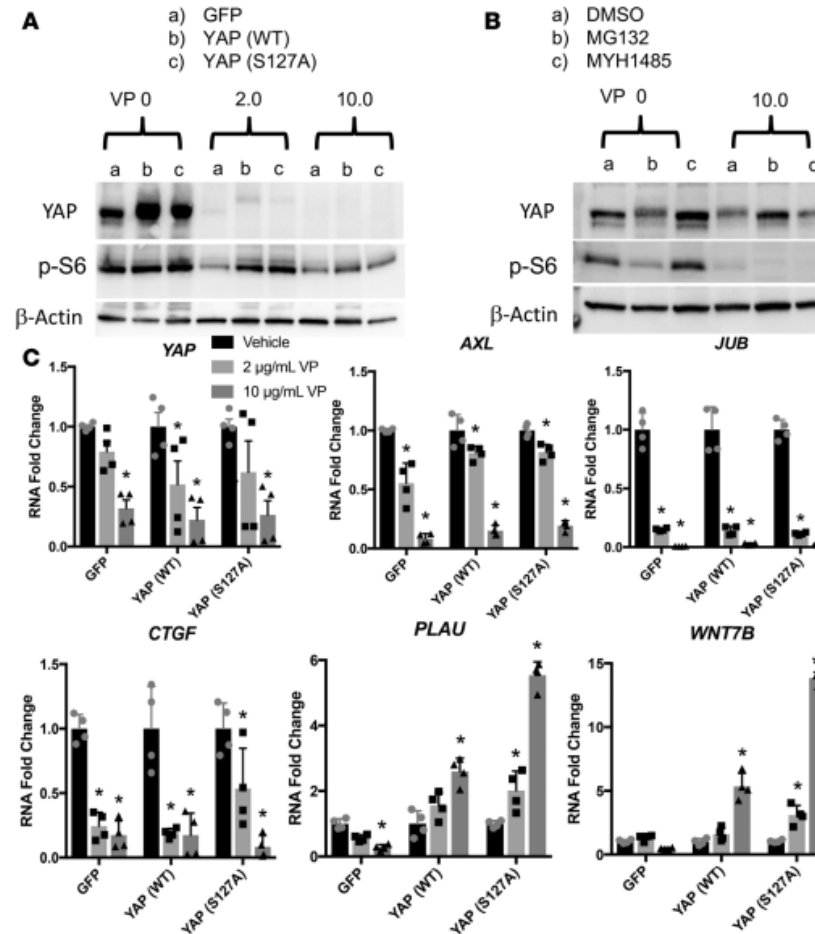


**Figure 7. Verteporfin reduces YAP transcriptional activity and phosphorylation of S6 in absence of light.** HBEC3s transfected with GFP, YAP (WT), or YAP (S127A) lentiviral vectors were treated with either vehicle (DMSO) or verteporfin (2.0 or 10.0  $\mu\text{g/ml}$ ) for 48 hours ( $n = 3$ ). **(A)** Western blot for YAP and p-S6 following a verteporfin dose curve in complete darkness show reduced total YAP and p-S6. **(B)** Western blot analysis of YAP and p-S6 following verteporfin treatment for 48 hours with MYH1485 treatment for the final 24 hours shows increased YAP after mTOR activation. Addition of MG132 for the final 24 hours of verteporfin treatment protects YAP from degradation caused by verteporfin. **(C)** *Yap*, *JUB*, *CTGF*, *AXL*, *PLAU*, and *WNT7B* RNAs were assessed in experiments performed in complete darkness ( $n = 4$  transfections). RNA expression is normalized to DMSO-treated cells.  $*P < 0.05$ , determined by ANOVA. HBEC3s, hTERT/CDK4-immortalized human bronchiolar epithelial cells.

# Results (8/8)

## *Temsirolimus blocks nuclear YAP, YAP-induced gene targets, cell proliferation and migration.*

- HBEC3s expressing YAP (WT) or YAP (S127A) were treated with temsirolimus (inhibitor of the mTOR pathway)
  - reduced YAP-mediated cell proliferation
  - inhibited phosphorylation of S6 and reduced nuclear YAP staining (Figure 8, A and B).
- Proteasome blocking with MG132 or activation of mTOR with MHY1485 did not prevent the loss of YAP by temsirolimus (Supplemental Figure 3D)
- Consistent with the inhibitory effect of temsirolimus on YAP activity, CTGF, JUB, and AXL were reduced (Figure 8C and Supplemental Figure 5)
- migration scratch assays were performed in HBEC3s expressing YAP (WT) and YAP (S127A)
  - Temsirolimus prevented YAP-induced cell migration in scratch assays (Figure 8D and Supplemental Figure 3A), supporting a network in which mTOR signaling cooperates with YAP to regulate epithelial cell migration and proliferation

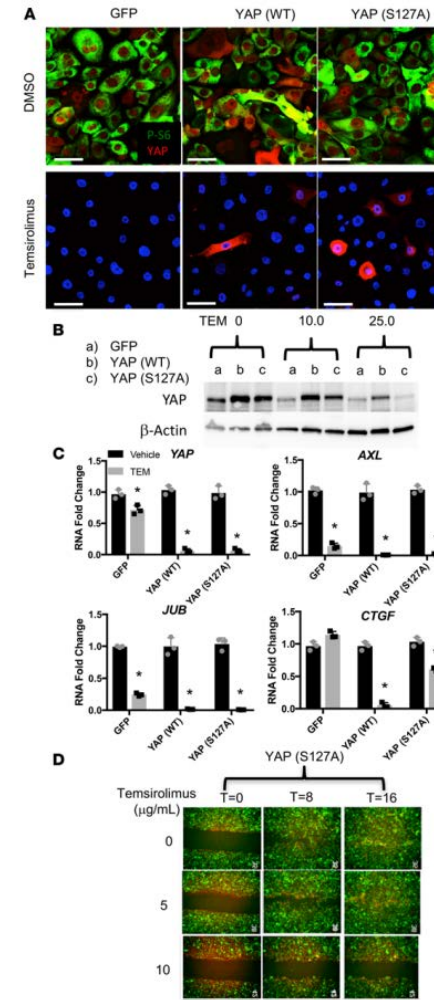


**Figure 8. Temsirolimus inhibits phosphorylation of S6, YAP transcriptional activity, and YAP-induced migration.** (A) Representative immunofluorescence microscopy was performed in HBEC3s transfected with GFP, YAP (WT), and YAP (S127A) and stained for p-S6 (green) and YAP (red) in the presence of temsirolimus (25 μg/ml) or DMSO (n = 5). Scale bars: 10 μm. (B) Western blot analysis of YAP following temsirolimus treatments shows reduced total YAP expression. (C) YAP, JUB, AXL, and CTGF RNAs were assessed after 48 hours (n = 3). RNA expression is normalized to DMSO-treated cells. (D) Time-lapse imaging of HBEC3s transfected with YAP (S127A) following treatment with temsirolimus at T = 0, 8, and 16 hours of a scratch assay (n = 3). \*P < 0.05, assessed by ANOVA. HBEC3s, hTERT/CDK4-immortalized human bronchiolar epithelial cells.

# Methods (1/1)

- **RNA analysis.** Comparative analysis of RNAs from sorted epithelial cells (CD326+/HTII-280+) from control (n = 3) and IPF donors (n = 3) (GSE94555) (15), and RNA sequences from primary HBECs expressing YAP (S127A) (19) were carried out to reveal commonly regulated pathways. Briefly, differentially expressed genes in IPF epithelial cells and in HBEC-YAP (S127A) were identified by Student's t test with FDR-adjusted P value < 0.05. Differentially expressed genes from the 2 data sets were subjected to gene set enrichment analysis using ToppGene Suite (<https://toppgene.cchmc.org/>), and commonly enriched bioprocesses and pathways were compared. Biological cross-talk and related networks among mTOR, PI3K/AKT, and Hippo/YAP signaling pathways were constructed using IPA (<http://www.ingenuity.com>). Regulatory relationships connecting gene nodes and cellular functions were identified through literature mining using the Ingenuity knowledge base. qPCR was used for validation, and RNA was extracted using the RNeasy Micro kit (Qiagen). cDNA was produced using an iScript cDNA synthesis kit (Bio-Rad). PCR was performed using a StepOne Plus RealTime PCR system (ABI 7500) utilizing TaqMan gene expression assays (Supplemental Table 2) (Applied Biosystems). All samples were assayed in duplicate for each target gene and quantification was performed using  $\Delta\Delta CT$  to determine gene fold changes.
- **Western blot.** Western blot was performed on human whole-tissue lysates obtained from resected normal donors, IPF, or COPD patient lungs. Diagnoses were made using criteria established by the American Thoracic Society and the European Respiratory Society to identify IPF and COPD samples postmortem. Control tissue was acquired from explanted lung from normal individuals with lungs rejected for transplant. Tissue lysates were prepared using RIPA buffer with protease and phosphatase inhibitors (MilliporeSigma) (19). Protein was measured using a Direct Detect infrared spectrometer (MilliporeSigma). Samples were run in a NOVEX 10%-20% Tris-glycine gel (Invitrogen). iBlot2 (Invitrogen) was used for dry transfer onto PVDF membranes (MilliporeSigma). Membranes were blocked using 5% bovine serum albumin (BSA) in Tris-buffered saline, 0.1% Tween 20 (TBST). Primary antibodies were diluted in 0.5% BSA/TBST. Western blots were quantified using Image Lab software (Bio Rad V5.2.1) and normalized to GAPDH or  $\beta$ -actin.
- **Immunofluorescence.** Immunofluorescence confocal microscopy was performed using paraffin-embedded samples with 5- $\mu$ m sections. Antigen retrieval in 10 mM citrate buffer (pH 6.0) or Tris-EDTA (pH 9.0) was used for some antibodies. Samples were blocked in 4% normal donkey serum in PBS, 0.1% Triton X-100 (PBST) for 1 hour. Slides were incubated in primary antibodies that were diluted in blocking buffer for 24-48 hours at 4°C. Antibody dilutions are listed in Supplemental Table 1. Samples were washed in PBST (3 times). Secondary antibody (1:200) and DAPI (1  $\mu$ g/ml) were added for 2 hours at room temperature. Samples were then washed in PBST, rinsed in phosphate buffer, and No. 1.5 cover slips were mounted with Prolong Gold (Thermo Fisher Scientific). Images were captured on an inverted Nikon A1R confocal microscope ( $\times 10$ ,  $\times 20$ , or  $\times 60$  magnification). Maximum intensity projections of Z-stack images were generated using NIS-Elements software (Nikon).
- **PLISH.** The PLISH protocol was provided by Tushar Desai, Stanford University, Stanford, California, USA (48). Paraffin sections were processed as described for immunofluorescence using antigen retrieval. RNA hybridization probes (100 nM) (Supplemental Table 3) were incubated in hybridization buffer (1 M sodium trichloroacetate, 5 mM EDTA, 50 mM Tris pH 7.4, 0.2 mg/ml heparin in DEPC water) for 2 hours at 37°C and 100% humidity. Sections were incubated with T4 ligase buffer (NEB) and phosphorylated common bridge and connector circle oligos (10 nM) for 60 minutes and followed with T4 ligase buffer and T4 ligase for 2 hours. NxGen phi29 DNA polymerase (Lucigen, 30221) was used for DNA amplification overnight. Slides were washed with label buffer (2 $\times$  SCC/20% formamide in DEPC water) and incubated with 100 nM Tye 705- or Alexa 568-labeled probe for 1 hour. Immunofluorescence costaining was performed and images obtained and analyzed as above. Reactions performed with probes for the Bacillus subtilis gene mgsA or mock reactions lacking hybridization probes were used for controls. Hybridization probes were ordered from Integrated DNA Technologies with standard desalting and stored as 100  $\mu$ M stocks.
- **Cell culture and lentiviral transduction.** HBEC3s were cultured and transduced as previously reported (19) using lentivirus (MOI = 1) containing SFFV-FLAG-hYAP-ires-eGFP (YAP), SFFV-FLAG-hYAP<sup>S127A</sup>-ires-eGFP (YAP S127A), or SFFV-ires-eGFP (control) (19). Verteporfin and temsirolimus stocks were resuspended in DMSO. For experiments conducted without ambient light, verteporfin stocks were prepared in the dark and all stages of cell culturing and sample collection were performed in the dark. Temsirolimus experiments were performed following standard culture protocols in ambient light. Cells were treated with verteporfin or temsirolimus for 48 hours. For immunofluorescence staining experiments, cells were cultured on ibiTreat chambered  $\mu$ -Slide coverslips (ibidi, 80826). For proteasome blocking studies, MG132 (2  $\mu$ M) (MilliporeSigma, M8699) or the mTOR activator MHY1485 (1  $\mu$ M) (MilliporeSigma, 500554), were added after 24 hours of exposure to verteporfin or temsirolimus. After 48 hours of verteporfin or temsirolimus and 24 hours of MG132 or MHY1485, protein lysates were collected for immunoblotting.
- **Cell count and viability.** A Muse Cell Analyzer and the Muse Cell Count and Viability assay were used (MilliporeSigma) to determine cell counts and viability, which were confirmed manually using trypan blue and a hemocytometer. For each experiment (n = 3) treatments were assessed in duplicate.
- **Cell migration assay.** HBEC3s transduced with control, YAP (WT), and YAP (S127A) cells were cultured on 48-well plates. At 100% confluence, cells were treated with DMSO, verteporfin, or temsirolimus. Scratches were performed using a P200 pipette tip. Time-lapse imaging of cell migration was recorded over 16 hours, with images captured every 10 minutes using a  $\times 10$  objective. Temsirolimus and control treatments were imaged on an inverted Nikon A1R LUNV confocal microscope. A SpectraX wide-field microscope with a long-pass filter (>680 nm) was used to image verteporfin experiments to minimize photo activation of the drug. For each experimental replicate (n = 3), n = 4 for each treatment.

# Discussion (1/3)

- IPF involves extensive remodeling of the peripheral lung parenchyma resulting in loss of alveolar gas exchange regions of the lung:
  - Normal alveoli, lined by AT1 and AT2 epithelial cells, are replaced by diverse pathological lesions lined by epithelial cells with abnormal conducting airway epithelial cell characteristics (goblet, ciliated, basal, and indeterminate cells in IPF) (5, 6, 15, 28)
- unbiased pathway analysis derived from RNAseq from CD326+/HT280+ sorted epithelial cells from IPF lungs and from primary HBECs expressing constitutively active YAP, indicated **activation of canonical signaling pathways regulated by Hippo/YAP and mTOR in both data sets**

# Discussion (2/3)

- Authors demonstrated increased nuclear YAP, YAP target gene expression, and S6 kinase activity in IPF epithelial cells – supporting the concept that YAP and mTOR signaling interact to influence epithelial cell shape, proliferation, and migration, processes that are likely to contribute to the pathogenesis of IPF (Figure 9).
- demonstrated that YAP and mTOR/ PI3K/AKT interact to influence cell proliferation and migration in HBEC3s
  - Phosphorylated PTEN was increased in IPF lung lysates, and expression of YAP (S127A) increased p-PTEN in HBEC3s, supporting a potential mechanism by which YAP activates mTOR signaling
  - p-S6K staining and p-S6 protein were increased in IPF epithelial cells and expression of YAP (S127A)-induced p-S6 in HBEC3s
  - Verteporfin inhibited YAP and reduced p-S6 staining in HBEC3s, demonstrating the direct interactions between the pathways.
  - temsirolimus inhibited YAP, YAP target genes - blocked YAP-induced increases in cell migration demonstrated a feed-forward signaling loop between YAP and mTOR
  - present findings that pharmacological activation of mTOR with MHY1485 induced YAP, temsirolimus decreased YAP, and expression of YAP (S127A) increases p-S6 in HBEC3s, provide evidence of a mechanism by which mTOR is both regulated by and regulates YAP activity in respiratory epithelial cells

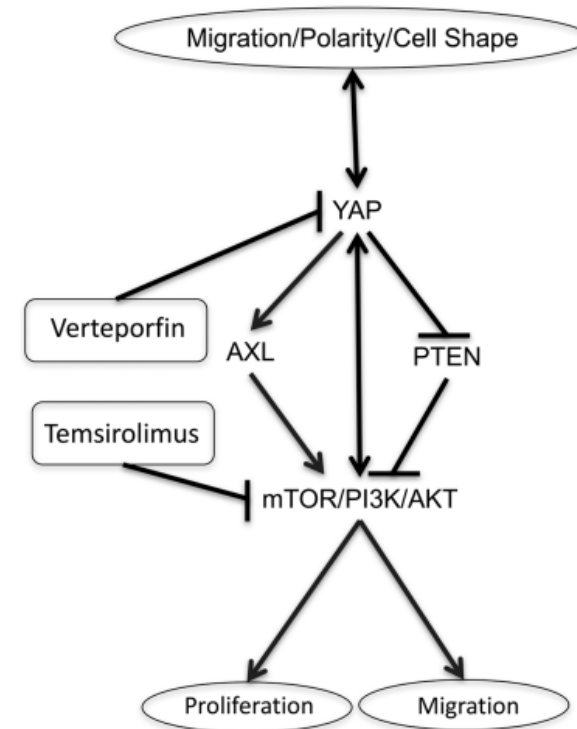


**Figure 9. Proposed polarity/YAP/mTOR network regulating epithelial cell processes.** Cell polarity is regulated by and regulates YAP activity. YAP expression alters cell shape. YAP (S127A) expression inhibits PTEN, increases AXL, and activates mTOR with increased p-S6, p-S6K, and p-PI3K. Blocking mTOR activity with temsirolimus inhibits YAP-induced cell proliferation and migration, and also reduces nuclear YAP staining. Verteporfin inhibits YAP nuclear localization and transcriptional activity, while reduced p-S6 staining indicates reduced mTOR.

## Discussion (3/3)

- Although initial clinical studies using mTOR inhibitors for treatment in IPF were unsuccessful, the present studies demonstrated extensive crosstalk between YAP and mTOR/PI3K/AKT
- They identified direct intersections between mTOR, YAP, and planar polarity pathways that together may influence cellular behaviors active in IPF.
- The present work identifies YAP/mTOR signaling components as potential prognostic and therapeutic targets for the treatment of IPF.

# References (1/2)

1. King TE, Pardo A, Selman M. Idiopathic pulmonary fibrosis. *Lancet*. 2011;378(9807):1949–1961. doi: 10.1016/S0140-6736(11)60052-4.
2. Steele MP, Schwartz DA. Molecular mechanisms in progressive idiopathic pulmonary fibrosis. *Annu Rev Med*. 2013;64:265–276. doi: 10.1146/annurev-med-042711-142004.
3. Barkauskas CE, Noble PW. Cellular mechanisms of tissue fibrosis. 7. New insights into the cellular mechanisms of pulmonary fibrosis. *Am J Physiol, Cell Physiol*. 2014;306(11):C987–C996.
4. Camelo A, Dunmore R, Sleeman MA, Clarke DL. The epithelium in idiopathic pulmonary fibrosis: breaking the barrier. *Front Pharmacol*. 2014;4:173.
5. Plantier L, et al. Ectopic respiratory epithelial cell differentiation in bronchiolised distal airspaces in idiopathic pulmonary fibrosis. *Thorax*. 2011;66(8):651–657.
6. Seibold MA, et al. The idiopathic pulmonary fibrosis honeycomb cyst contains a mucociliary pseudostratified epithelium. *PLoS ONE*. 2013;8(3):e58658.
7. Kropski JA, Blackwell TS, Loyd JE. The genetic basis of idiopathic pulmonary fibrosis. *Eur Respir J*. 2015;45(6):1717–1727.
8. Wang Y, et al. Genetic defects in surfactant protein A2 are associated with pulmonary fibrosis and lung cancer. *Am J Hum Genet*. 2009;84(1):52–59.
9. Nogee LM, Dunbar AE, Wert S, Askin F, Hamvas A, Whitsett JA. Mutations in the surfactant protein C gene associated with interstitial lung disease. *Chest*. 2002;121(3 Suppl):20S–21S.
10. Nogee LM, Dunbar AE, Wert SE, Askin F, Hamvas A, Whitsett JA. A mutation in the surfactant protein C gene associated with familial interstitial lung disease. *N Engl J Med*. 2001;344(8):573–579.
11. Whitsett JA, Wert SE, Weaver TE. Diseases of pulmonary surfactant homeostasis. *Annu Rev Pathol*. 2015;10:371–393.
12. Li M, et al. Epithelium-specific deletion of TGF- $\beta$  receptor type II protects mice from bleomycin-induced pulmonary fibrosis. *J Clin Invest*. 2011;121(1):277–287.
13. Bonniaud P, et al. Smad3 null mice develop airspace enlargement and are resistant to TGF-beta-mediated pulmonary fibrosis. *J Immunol*. 2004;173(3):2099–2108.
14. Chang W, et al. A critical role for the mTORC2 pathway in lung fibrosis. *PLoS One*. 2014;9(8):e106155.:1335–1345.

# References (2/2)

15. Xu Y, et al. Single-cell RNA sequencing identifies diverse roles of epithelial cells in idiopathic pulmonary fibrosis. *JCI Insight*. 2016;1(20):e90558.
16. Pflieger CM. The Hippo pathway: A master regulatory network important in development and dysregulated in disease. *Curr Top Dev Biol*. 2017;123:181–228.
17. Shimomura T, Miyamura N, Hata S, Miura R, Hirayama J, Nishina H. The PDZ-binding motif of Yes-associated protein is required for its co-activation of TEAD-mediated CTGF transcription and oncogenic cell transforming activity. *Biochem Biophys Res Commun*. 2014;443(3):917–923.
18. Cui ZL, et al. YES-associated protein 1 promotes adenocarcinoma growth and metastasis through activation of the receptor tyrosine kinase Axl. *Int J Immunopathol Pharmacol*. 2012;25(4):989–1001.
19. Lange AW, Sridharan A, Xu Y, Stripp BR, Perl AK, Whitsett JA. Hippo/Yap signaling controls epithelial progenitor cell proliferation and differentiation in the embryonic and adult lung. *J Mol Cell Biol*. 2015;7(1):35–47.
20. Das Thakur M, Feng Y, Jagannathan R, Seppa MJ, Skeath JB, Longmore GD. Ajuba LIM proteins are negative regulators of the Hippo signaling pathway. *Curr Biol*. 2010;20(7):657–662.
21. Zhao B, Tumaneng K, Guan KL. The Hippo pathway in organ size control, tissue regeneration and stem cell self-renewal. *Nat Cell Biol*. 2011;13(8):877–883. [insight.jci.org](https://doi.org/10.1172/jci.insight.98738)  
<https://doi.org/10.1172/jci.insight.98738>
22. Varelas X. The Hippo pathway effectors TAZ and YAP in development, homeostasis and disease. *Development*. 2014;141(8):1614–1626.
23. Volckaert T, et al. Fgf10-Hippo epithelial-mesenchymal crosstalk maintains and recruits lung basal stem cells. *Dev Cell*. 2017;43(1):48–59.e5.
24. Lin C, et al. YAP is essential for mechanical force production and epithelial cell proliferation during lung branching morphogenesis. *Elife*. 2017;e21130.
25. Mahoney JE, Mori M, Szymaniak AD, Varelas X, Cardoso WV. The hippo pathway effector Yap controls patterning and differentiation of airway epithelial progenitors. *Dev Cell*. 2014;30(2):137–150.
26. Zhao R, et al. Yap tunes airway epithelial size and architecture by regulating the identity, maintenance, and self-renewal of stem cells. *Dev Cell*. 2014;30(2):151–165.
27. Brodowska K, et al. The clinically used photosensitizer Verteporfin (VP) inhibits YAP-TEAD and human retinoblastoma cell growth in vitro without light activation. *Exp Eye Res*. 2014;124:67–73.
28. Chilosi M, et al. Abnormal re-epithelialization and lung remodeling in idiopathic pulmonary fibrosis: the role of deltaN-p63. *Lab Invest*. 2002;82(10):1335–1345.